Available online at www.sciencedirect.com
SCIENCE DIRECT
Journal of Sound and Vibration 294 (2006) 1060–1072
JOURNAL OF SOUND AND VIBRATION
www.elsevier.com/locate/jsvi

Timoshenko beam model for vibration analysis of multi-walled carbon nanotubes

C.M. Wang[a,*], V.B.C. Tan[b], Y.Y. Zhang[b]

[a]Department of Civil Engineering, National University of Singapore, Kent Ridge, Singapore 119260, Singapore
[b]Department of Mechanical Engineering, National University of Singapore, Kent Ridge, Singapore 119260, Singapore

Received 19 July 2004; received in revised form 9 December 2004; accepted 7 January 2006
Available online 9 March 2006

Abstract

This paper is concerned with the use of the Timoshenko beam model for free vibration analysis of multi-walled carbon nanotubes (CNTs). Unlike the Euler beam model, the Timoshenko beam model allows for the effects of transverse shear deformation and rotary inertia. These effects become significant for CNTs with small length-to-diameter ratios that are normally encountered in applications such as nanoprobes. By using the differential quadrature (DQ) method, the governing Timoshenko equations are solved for CNTs of different length-to-diameter ratios and boundary conditions. By comparing results based on the Timoshenko and the Euler beam theories, we show that the frequencies are significantly overpredicted by the Euler beam theory when the length-to-diameter ratios are small and when considering high vibration modes. For such situations, the Timoshenko beam model should be used for a better prediction of the frequencies.

1. Introduction

In recent years, researchers have advanced the field of nanotechnology at a phenomenal pace. In particular, the discovery of carbon nanotubes (CNTs) in 1991 [1] has speeded the development of nanotechnology because these CNTs possess superior mechanical, electronic and chemical properties [2–5]. They are about ten times stronger but six times lighter than steel [6]. They can conduct electricity as a semiconductor and transmit heat extremely well. Undoubtedly, CNTs holds great potential in becoming the new nanomaterial of this early part of the 21st century.

The mechanical behavior of CNTs has been explored through experiments, molecular dynamics (MD) simulations, and elastic continuum mechanics. Presently there are some difficulties encountered in conducting experiments on CNTs because of the nanometer dimensions. MD simulations are highly computationally time consuming and have often been limited to coarse atomic systems. The search for more practical and cost effective analysis methods is on. It is reported in the literature that continuum mechanics may serve as an alternative method to study CNTs instead of MD and experiments by treating CNTs as continuum elastic structures. By studying the buckling of single-walled nanotubes and comparing the results of atomic modeling

*Corresponding author. Tel.: +65 874 2157; fax: +65 779 1635.
E-mail address: cvewcm@nus.edu.sg (C.M. Wang).

0022-460X/$ - see front matter © 2006 Elsevier Ltd. All rights reserved.
doi:10.1016/j.jsv.2006.01.005

with a continuum shell model, Yakobson et al. [7] found that the continuum shell model can be used to estimate all the changes of buckling patterns satisfactorily. Their studies together with many others lead to the conclusion that "The laws of continuum mechanics are amazingly robust and allow one to treat even intrinsically discrete objects only a few atoms in diameter" [8]. In recent years, many elastic continuum models were developed including beam models [9,10], cylindrical shell models [11–15] and space truss/frame models [16,17] for studying the bending, buckling and vibration behaviors of CNTs.

Based on a literature search, it is observed that the Euler beam model is widely used in vibration and buckling analyses [2,10,18,19] and in sound wave propagation problems [20,21]. The simplicity of the single elastic beam model, which neglects the interaction between tubes and assumes that the nested tubes of multi-walled carbon nanotubes (MWNTs) deform coaxially, has led to its numerous applications in static and dynamic studies of MWNTs [2,18,23–25]. For instance, for the vibration of MWNTs embedded in an elastic medium, a single elastic beam model has been shown to be adequate in predicting the frequency of double-walled CNT of very large length-to-diameter ratios [10].

The single Euler beam (SEB) model is relatively simple and easy to apply. The governing equation of Euler beams contains only one unknown variable (the deflection of the beam) because the effects of transverse shear deformation and rotary inertia are ignored. However, these effects do have a substantial effect on the vibration frequencies of CNTs when the tubes are stocky and when dealing with high modes of vibration. Stocky beams are encountered when CNTs are applied as nanotweezers [26] and nanoprobes [27–29] since they generally have small length-to-diameter ratios. When investigating the dynamics responses of nanotubes in elastic medium using the modal expansion technique, one requires a large number of vibration modes including the high modes for accurate responses. Furthermore, the study of high modes of vibration is important in order to avoid the destructive effect of resonance occurring at high frequencies. Therefore, to capture more accurately the mechanical behavior of CNTs, we propose that the Timoshenko beam model be utilized rather than the Euler beam model. Yoon et al. [22] is probably one of the earliest researchers to use the Timoshenko beam model for CNTs. They used the model to study the effects of shear deformation and rotary inertia on wave propagation in CNTs.

In this paper, the free vibration behavior of MWNTs is investigated using the Timoshenko beam model. The effects of shear deformation and rotary inertia on the vibration frequencies are examined for different length-to-diameter ratios of CNTs under various end conditions. The differential quadrature (DQ) method is applied to solve the coupled governing vibration equations of the MWNTs.

In the treatment of a MWNT using the Timoshenko beam model, we can either have a single-Timoshenko beam (STB) to model the MWNT or a multi-Timoshenko beam model where each beam models one carbon nanotube of the multi-walled CNTs. We begin this study with the STB model as it will elucidate the Timoshenko beam equations and the DQ method for solution. These equations will later be augmented for the multi-Timoshenko beam model and a double-walled CNT is solved so as to investigate the effects of transverse shear deformation and rotary inertia on the frequencies.

2. STB model

2.1. Basic equations

The governing equations for a vibrating Timoshenko beam are given by Timoshenko [30]

$$\rho A\omega^2 w - KGA\left(\frac{\mathrm{d}\varphi}{\mathrm{d}x} - \frac{\mathrm{d}^2 w}{\mathrm{d}x^2}\right) = 0, \tag{1a}$$

$$EI\frac{\mathrm{d}^2\varphi}{\mathrm{d}x^2} - KGA\left(\varphi - \frac{\mathrm{d}w}{\mathrm{d}x}\right) + \rho I\omega^2\varphi = 0, \tag{1b}$$

where w is the transverse displacement, φ the slope of the beam due to bending deformation alone, x the axial coordinate, I the second moment of area of cross-section, A the cross-sectional area, ρ the mass density per

unit volume, K the shear correction factor, E the Young's modulus, G the shear modulus and ω the circular frequency of the beam.

2.2. DQ formulation

The analytical solutions for Eq. (1) for Timoshenko beams with various boundary conditions are available in the literature (e.g. Ref. [31]). We shall use these analytical solutions to verify the results obtained by the DQ method. For more information on the DQ method, readers may refer to Ref. [32]. The essence of DQ method is that the partial derivative of a function with respect to a space variable at a grid point can be approximated as the weighted linear sum of the function values at all grid points in the whole domain. The computational domain of the beam is $0 \leqslant x \leqslant L$. We assume that the beam is divided into $(M-1)$ intervals by M grid points with the coordinates given as $x_1, x_2, \ldots, x_M$. Here we adopt the well accepted mesh point distribution [32]

$$x_i = \frac{1}{2}\left[1 - \cos\left(\frac{i-1}{M-1}\pi\right)\right] \times L, \quad i = 1, 2, \ldots, M. \tag{2}$$

By applying the DQ rule to Eqs. (1a) and (1b) in the beam domain $0 \leqslant x \leqslant L$, one obtains the following discretized formulation of Eqs. (1a) and (1b):

$$KGA \sum_{j=1}^{M} b_{ij} w_j + \rho A \omega^2 w_i - KGA \sum_{j=1}^{M} a_{ij} \varphi_j = 0, \tag{3a}$$

$$EI \sum_{j=1}^{M} b_{ij} \varphi_j - (KGA - \rho I \omega^2)\varphi_i + KGA \sum_{j=1}^{M} a_{ij} w_j = 0, \tag{3b}$$

where $i = 1, \ldots, M$ and a_{ij}, b_{ij} are the weighting coefficients for the grid point at x_i of the first- and second-order derivatives, respectively. The weighting coefficients can be calculated on the basis of Eq. (2). Their explicit expressions are given in Appendix A.

2.3. Eigenvalue equation

In view of the boundary conditions, Eqs. (3a) and (3b) can be expressed in the following matrix form:

$$[\mathbf{S}]\{\mathbf{U}\} = \omega^2 \{\mathbf{U}\}, \tag{4}$$

where $\{\mathbf{U}\}^{\mathrm{T}} = \{w_2, w_3, \ldots, w_{M-1}, \varphi_2, \varphi_3, \ldots, \varphi_{M-1}\}$ including the degrees of freedom on the interior points of the domain and $[\mathbf{S}]$ is the stiffness matrix.

The natural vibration frequencies of the beam are furnished by the eigenvalues of the eigenvalue problem defined by Eq. (4). The eigenvalues may be computed using any standard eigenvalue solver such as the QR algorithm [33].

2.4. Example problems

Let us consider a double-walled CNT with an inner diameter $2R_1 = 0.7\,\mathrm{nm}$ and an outer diameter $d = 2R_2 = 1.4\,\mathrm{nm}$, where R_1 is the radius of the inner tube centreline while R_2 is the radius of the outer tube centerline [10,28,29]. The CNT is either clamped at both ends (CC) as shown in Fig. 1 or clamped at one end and free at the other end (CF). It is assumed that the inner and outer tubes have the same Young's modulus $E = 1\,\mathrm{TPa}$ (with the effective thickness of single-walled CNTs $t = 0.35\,\mathrm{nm}$), shear modulus $G = 0.4\,\mathrm{TPa}$, Poisson's ratio $v = 0.25$ [10]. In accordance to the definition of the effective thickness and the Young's modulus mentioned above, a mass density $\rho = 2.3\,\mathrm{g/cm^3}$ is adopted [22]. The cross-sectional area A and moment of inertia I are the total cross-sectional area and the total moment of inertia of double-walled CNT, i.e. $A = A_1 + A_2$ and $I = I_1 + I_2$ where the subscripts 1, 2 are used to denote the quantities belonging to the inner and outer tubes, respectively. Since the present double-walled CNT is treated as a single beam with hollow annular cross section, the dependence of the shear correction factor K on its cross-sectional shape is

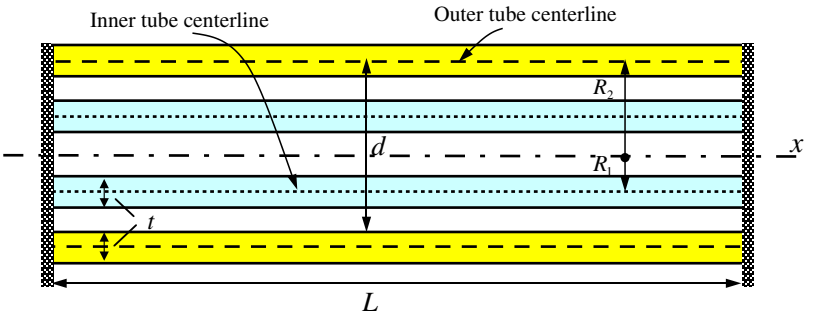

Fig. 1. Geometry of double-walled CNT.

Table 1
Frequency parameter $\Omega = \sqrt[4]{\rho A\omega_n^2 L^4/(EI)}$ of CC double-walled CNT modeled by STB and SEB models

Mode number n	STB				SEB
	$L/d = 10$	$L/d = 30$	$L/d = 50$	$L/d = 100$	
1	4.5533	4.7085	4.7222	4.7280	4.7300
2	7.2493	7.7718	7.8234	7.8457	7.8540
3	9.6978	10.799	10.922	10.977	10.995
4	11.900	13.755	13.992	14.100	14.137
5	13.898	16.630	17.028	17.214	17.279
6	15.7270	19.420	20.025	20.317	20.420
7	17.4153	22.119	22.978	23.408	23.561
8	18.985	24.726	25.884	26.484	26.703
9	20.454	27.244	28.740	29.544	29.845
10	21.833	29.674	31.544	32.588	32.987

considered, and K is determined by the following formula [34]:

$$K = \frac{6(1+\nu)(1+\alpha)^2}{(7+6\nu)(1+\alpha)^2 + (20+12\nu)\alpha^2}, \tag{5}$$

where $\alpha = (2R_1 - t)/(2R_2 + t)$ is the ratio of the innermost and the outermost diameters of the tube. By substituting the adopted values of R_1, R_2 and ν into Eq. (5), we obtain $K = 0.82$.

Using the DQ method, we compute the first ten natural frequency parameters $\Omega = \sqrt[4]{\rho A\omega_n^2 L^4/(EI)}$ where n is the mode number for both sets of boundary conditions. The results for CC beams and CF beams are tabulated in Tables 1 and 2, respectively, for various length-to-diameter ratios. These results are compared with the corresponding results based on a SEB model [30]. The latter results are computed from these characteristic equations:

$$\cosh(\Omega)\cos(\Omega) = 1 \text{ for CC beam}, \tag{6}$$

$$\cosh(\Omega)\cos(\Omega) = -1 \text{ for CF beam}. \tag{7}$$

From the results shown in Tables 1 and 2, it can be observed that for stocky CNTs, i.e. relatively small length-to-diameter ratios ($L/d \leqslant 30$), the vibration results of the Timoshenko beam model are significantly lower than the Euler beam model results due to the effects of shear deformation and rotary inertia. For example, the Euler beam model overpredicts the frequencies of CC double-walled CNT with $L/d = 10$ by 3.735%, 19.56% and 33.81% for the 1st, 5th and 10th mode, respectively. The relative percentage difference in the results from the two beam models increases with respect to increasing mode numbers.

Table 2
Frequency parameter $\Omega = \sqrt[4]{\rho A \omega_n^2 L^4/(EI)}$ of CF double-walled CNT modeled by STB and SEB models

Mode number n	STB				SEB
	$L/d = 10$	$L/d = 30$	$L/d = 50$	$L/d = 100$	
1	1.8663	1.8741	1.8747	1.8750	1.8750
2	4.5503	4.6769	4.6878	4.6925	4.6940
3	7.3437	7.7872	7.8300	7.8485	7.8539
4	9.8415	10.824	10.932	10.979	10.995
5	12.090	13.795	14.008	14.104	14.137
6	14.122	16.688	17.051	17.220	17.279
7	15.973	19.496	20.057	20.326	20.420
8	17.671	22.214	23.019	23.419	23.562
9	19.238	24.841	25.936	26.498	26.703
10	20.690	27.377	28.802	29.562	29.845

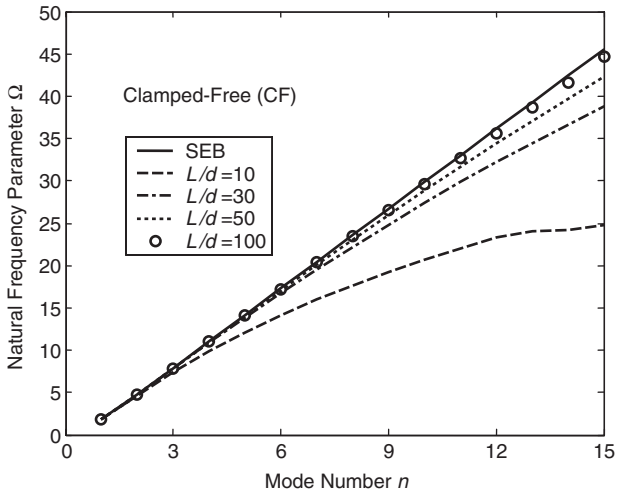

Fig. 2. Comparison of results between SEB and STB models for CC double-walled CNT.

For long and slender CNTs (i.e. $L/d > 50$), the effects of shear deformation and rotary inertia on the vibration frequencies are negligible as can be observed from the Timoshenko and Euler beam results in Tables 1 and 2. This can also be observed from the frequency values with respect to the mode number in Figs. 2 and 3. Note that the close agreement of frequencies obtained by the DQ method and by Eqs. (6) and (7) for $L/d = 100$ verifies the correctness of the DQ formulation.

However, it should be pointed out that the single beam model fails to represent the behavior of individual tubes and the relative deformation between adjacent tubes. For example, the single beam model provides only one set of n-order frequencies for double-walled CNTs when there should be two sets due to non-coaxial vibration. Another obvious drawback of the model is that it is only applicable when both nested tubes have the same end conditions. It is possible for the nanotubes in a double-walled CNT to have different boundary conditions. In this case, the single beam model cannot model such boundary conditions and a more refined double-beam model is needed. It is clear that for MWNTs, we need a multi-beam model.

3. Multi-walled Timoshenko beam model

A multi-beam model has been developed and applied for the analysis of buckling [35] and free vibration of MWNTs [10]. In the aforementioned papers, the multi-beam model is based on the Euler beam theory and

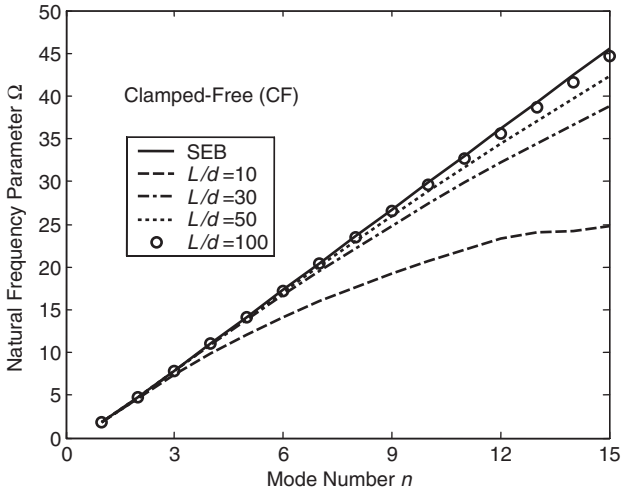

Fig. 3. Comparison of results between SEB and STB models for CF double-walled CNT.

assumes that all the nested, concentric single-walled CNT are described by an elastic beam individually. In the multi-beam model, the deflections of the adjacent tubes are coupled due to the presence of the so-called van der Waals forces. The forces are modeled by a Winkler-type model involving the relative interlayer radial displacements. Since the nanotubes are treated individually in the multi-beam model, the end conditions can therefore be described individually. Thus, the improved model can be adopted to simulate MWNTs with tubes having different end conditions. In contrast to the single beam model, the multi-beam model is a better one since it can take into consideration (a) van der Waals forces, (b) different boundary conditions for each nanotube of the MWNT and (c) provides N sets of frequencies, where N is the number of the nanotubes in a MWNT.

As an improvement of the multi-Euler beam model, the multi-Timoshenko beam model is proposed. In this model, each nanotube of aMWNT is simulated by a Timoshenko beam that allows for the effects of transverse shear deformation and rotary inertia. The deflections of the adjacent tubes are coupled through the van der Waals force which is determined by the interlayer spacing. By augmenting Eq. (1) for a MWNT with N tubes, the $2 \times N$ coupled governing equations are:

$$\rho A_1\omega^2 w_1 - K_1 G A_1\left(\frac{\mathrm{d}\varphi_1}{\mathrm{d}x} - \frac{\mathrm{d}^2 w_1}{\mathrm{d}x^2}\right) = -c_1(w_2 - w_1),$$
$$EI_1\frac{\mathrm{d}^2\varphi_1}{\mathrm{d}x^2} - K_1 G A_1\left(\varphi_1 - \frac{\mathrm{d}w_1}{\mathrm{d}x}\right) + \rho I_1\omega^2\varphi_1 = 0, \tag{8a}$$

$$\rho A_2\omega^2 w_2 - K_2 G A_2\left(\frac{\mathrm{d}\varphi_2}{\mathrm{d}x} - \frac{\mathrm{d}^2 w_2}{\mathrm{d}x^2}\right) = -c_2(w_3 - w_2) + c_1(w_2 - w_1),$$
$$EI_2\frac{\mathrm{d}^2\varphi_2}{\mathrm{d}x^2} - K_2 G A_2\left(\varphi_2 - \frac{\mathrm{d}w_2}{\mathrm{d}x}\right) + \rho I_2\omega^2\varphi_2 = 0,$$
$$\vdots \tag{8b}$$

$$\rho A_N\omega^2 w_N - K_N G A_N\left(\frac{\mathrm{d}\varphi_N}{\mathrm{d}x} - \frac{\mathrm{d}^2 w_N}{\mathrm{d}x^2}\right) = c_{N-1}(w_N - w_{N-1}),$$
$$EI_N\frac{\mathrm{d}^2\varphi_N}{\mathrm{d}x^2} - K_N G A_N\left(\varphi_N - \frac{\mathrm{d}w_N}{\mathrm{d}x}\right) + \rho I_N\omega^2\varphi_N = 0, \tag{8n}$$

where I_j is the second moment of area of the jth tube, A_j the cross-sectional area of jth tube, and K_j the shear correction factor of the jth tube. Since each of the tube of the MWNT is modeled by an individual Timoshenko beam. The shear correction factors K_j of these beams/tubes are different from each other according to Eq. (5) due to their different cross-sectional dimensions. In addition, it is assumed that all tubes share the same Young's modulus, shear modulus and mass density. The van der Waals interaction coefficients $c_j (j = 1, 2, \ldots, N-1)$ can be estimated as [6]

$$c_j = \frac{320 \times (2R_j)\text{erg/cm}^2}{0.16\Delta^2}, \quad \Delta = 0.142\,\text{nm}, \quad j = 1, 2, \ldots, N-1, \tag{9}$$

where R_j is the center line radius of the jth tube and Δ the length of carbon–carbon (C–C) bond. For the present double-walled CNT with $R_1 = 0.35\,\text{nm}$, Eq. (9) gives $c_1 = 6.943 \times 10^{11}\,\text{erg/cm}^3 = 0.06943\,\text{TPa}$.

In this study, the MWNTs modeled according to the Timoshenko beam theory are free of the surrounding elastic medium, i.e. free of external lateral pressure. However, this lateral pressure effect can be easily accommodated by adding the term kw_N in the right-hand side of the first equation in Eq. (8n), where k is the spring constant determined by the material constants of the elastic medium, the outermost diameter of the embedded MWNT, and the wave-length of vibrational modes [10].

3.1. Double-Timoshenko beam (DTB) model for double-walled CNT

Using Eq. (7) with $N = 2$ and the DQ rule, the discretized governing equations for double-walled CNT are:

$$\begin{aligned} &K_1GA_1\sum_{j=1}^{M} b_{ij}w_{1j} - c_1w_{2i} + (c_1 - \rho A_1\omega^2)w_{1i} - K_1GA_1\sum_{j=1}^{M} a_{ij}\varphi_{1j} = 0,\\ &EI_1\sum_{j=1}^{M} b_{ij}\varphi_{1j} + (\rho I_1\omega^2 - K_1GA_1)\varphi_{1i} + K_1GA_1\sum_{j=1}^{M} a_{ij}w_{1j} = 0, \end{aligned} \tag{10a}$$

$$\begin{aligned} &K_2GA_2\sum_{j=1}^{M} b_{ij}w_{2j} - c_1w_{1i} + (c_1 - \rho A_2\omega^2)w_{2i} - K_2GA_2\sum_{j=1}^{M} a_{ij}\varphi_{2j} = 0,\\ &EI_2\sum_{j=1}^{M} b_{ij}\varphi_{2j} + (\rho I_2\omega^2 - K_2GA_2)\varphi_{2i} + K_2GA_2\sum_{j=1}^{M} a_{ij}w_{2j} = 0 \end{aligned} \tag{10b}$$

for $i = 1, 2, \ldots, M$. The subscripts 1 and 2 denote the quantities of the inner and outer tubes, respectively. Based on Eq. (5) and the adopted values of R_1, R_2 and v, we obtain $K_1 = 0.75$ and $K_2 = 0.64$ for the inner tube and the outer tube, respectively.

For our calculations, the double-walled CNT is assumed to have the same geometrical and material parameters that are given in Section 2. The influences of transverse shear deformation and rotary inertia on the vibration frequencies are investigated by comparing the double-Timoshenko beam (DTB) results to those based on the Euler beam model. The analytical results based on the double-Euler beam (DEB) model for the free vibration of double-walled CNT are reported in the paper by Yoon et al. [10]. In their paper [10], the two sets of n-order resonant frequencies are given by

$$\omega_{n1}^2 = \tfrac{1}{2}\left(\alpha_n - \sqrt{\alpha_n^2 - 4\beta_n}\right), \tag{11a}$$

$$\omega_{n2}^2 = \tfrac{1}{2}\left(\alpha_n + \sqrt{\alpha_n^2 - 4\beta_n}\right), \tag{11b}$$

where

$$\alpha_n = \Omega_n^4\left[\frac{EI_1}{\rho A_1 L^4} + \frac{EI_2}{\rho A_2 L^4}\right] + c_1\frac{A}{\rho A_1 A_2}, \tag{12a}$$

$$\beta_n = \Omega_n^8\left[\frac{EI_1}{\rho A_1 L^4}\frac{EI_2}{\rho A_2 L^4}\right] + c_1\Omega_n^4\left(\frac{EI_1}{\rho A_1 L^4} + \frac{EI_2}{\rho A_2 L^4}\right), \tag{12b}$$

where $A = A_1 + A_2$.

Figs. 4 and 5 compare the frequencies obtained by DTB and DEB models for various length-to-diameter ratios and for CC and CF end conditions. In the figures, the lower frequency parameter set is defined as $\Omega_{n1} = \sqrt[4]{\omega_{n1}^2 \rho A L^4/(EI)}$ while the higher set by $\Omega_{n2} = \sqrt[4]{\omega_{n2}^2 \rho A L^4/(EI)}$ where $I = I_1 + I_2$.

From Fig. 4, we observe that for small length-to-diameter ratios, for instance $L/d = 10$, the effects of shear deformation and rotary inertia on the frequency values cannot be ignored, especially for higher modes. It is clearly seen from Fig. 4a that shear deformation and rotary inertia lead to a significant reduction in the frequencies. With increasing length-to-diameter ratios, say $L/d = 30$ and beyond, the effects of shear deformation and rotary inertia on the frequencies diminish at lower modes but are still somewhat significant at higher modes. As shown in Fig. 4b, the Euler and the Timoshenko results for the lower set of n-order resonant frequencies are in good agreement when $n \leqslant 5$ and for the higher set of frequencies when $n \leqslant 9$. Beyond these n values, the Timoshenko results are lower than their Euler counterparts and their differences increase with increasing n values. It is clear that shear deformation and rotary inertia have more influence on the lower set of n-order resonant frequencies Ω_{n1}.

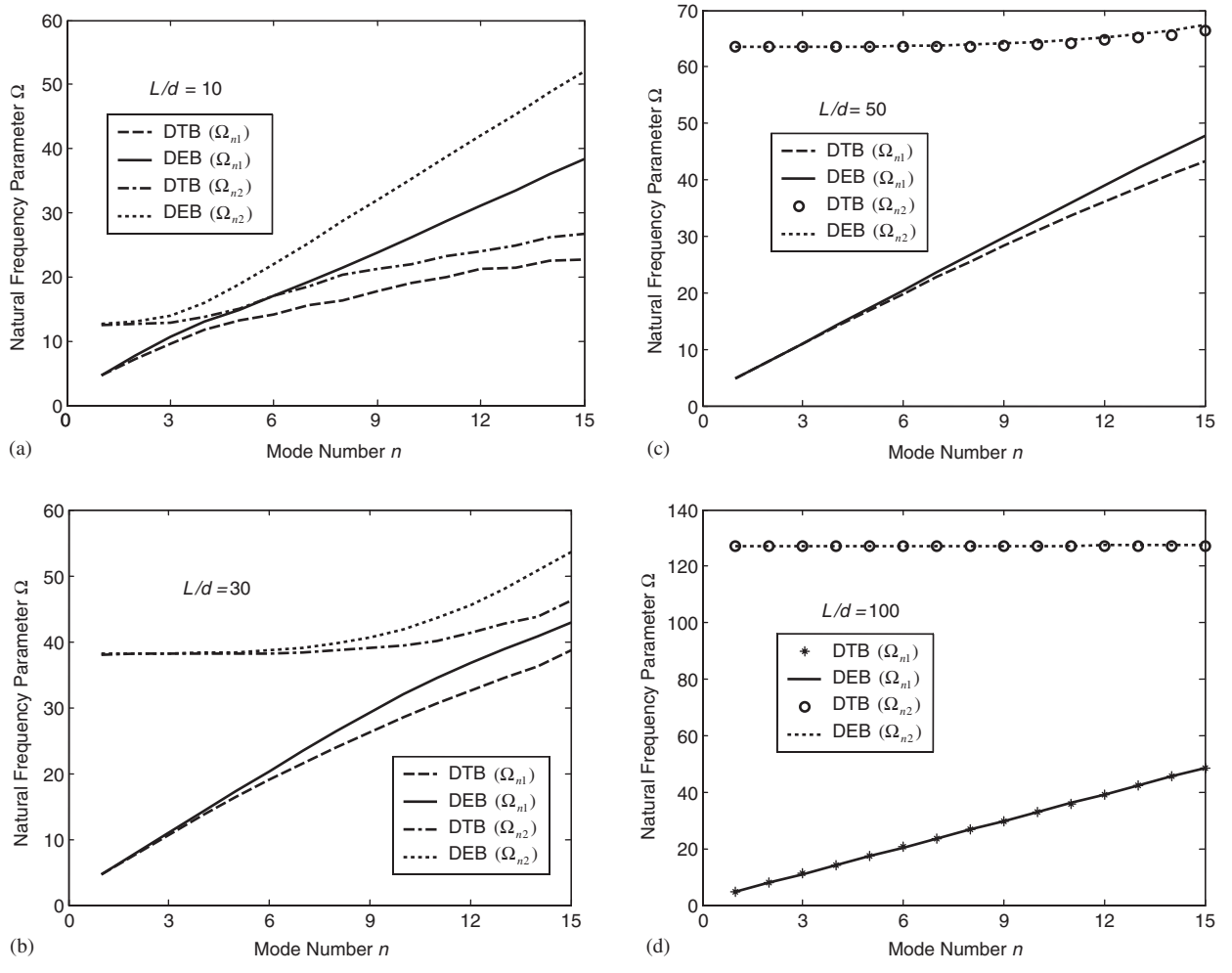

Fig. 4. Frequencies of CC double-walled CNT against mode number n based on DTB and DEB models (a) $L/d = 10$; (b) $L/d = 30$; (c) $L/d = 50$; (d) $L/d = 100$.

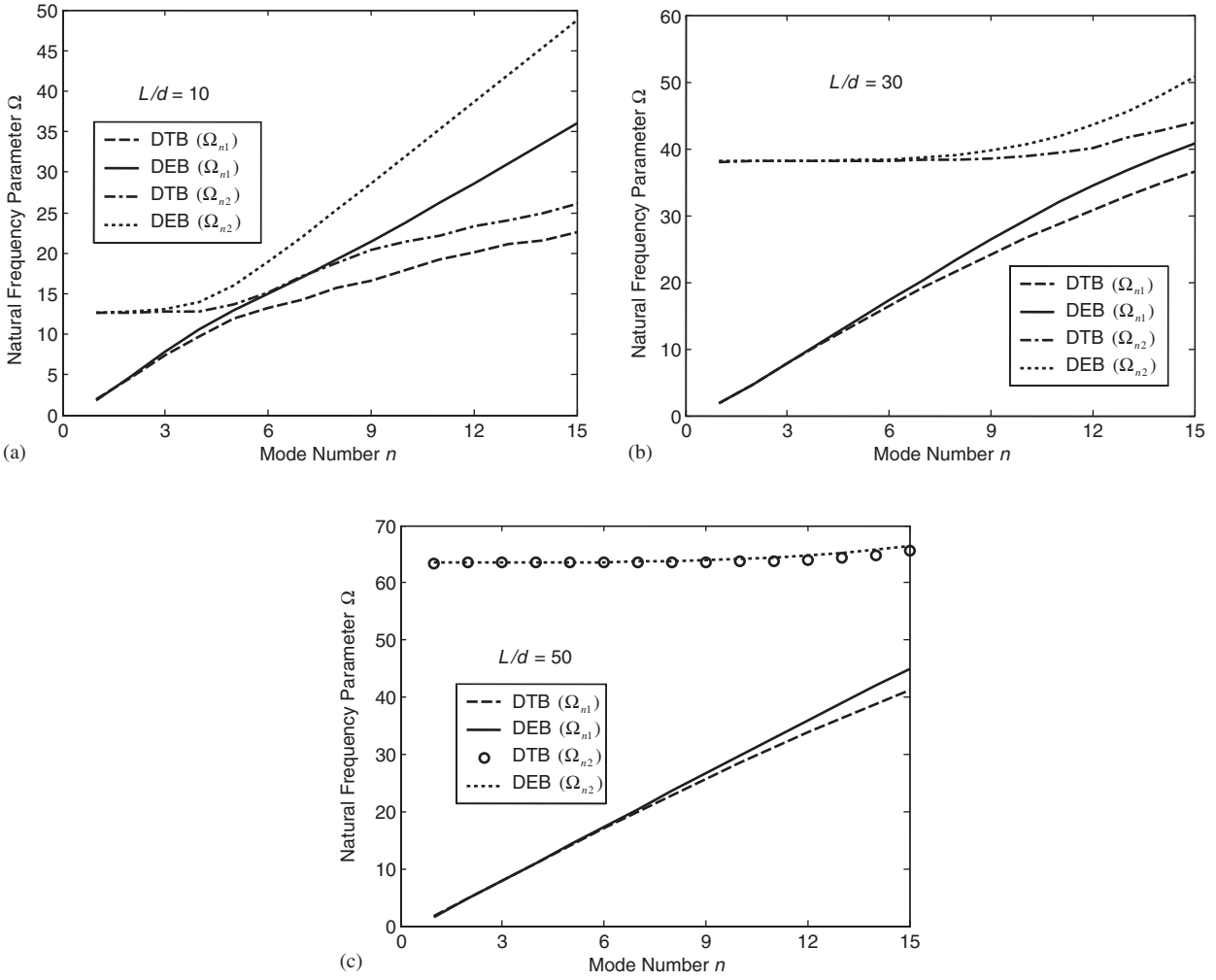

Fig. 5. Frequencies of CF double-walled CNT against mode number n based on DTB and DEB models (a) $L/d = 10$; (b) $L/d = 30$; (c) $L/d = 50$.

For the higher set of frequencies, the frequency values do not vary much with respect to the mode number as well as L/d when this ratio is greater than 30. This constancy of frequency set can be obtained from Eqs. (11b), (12a) and (12b). For large values of L/d and small n values, we can argue that $L^4/I_1 \gg \Omega_n^4$ and $L^4/I_2 \gg \Omega_n^4$, and therefore Eqs. (12a) and (12b) become

$$\alpha_n \to \frac{c_1}{\rho A_1} + \frac{c_1}{\rho A_2} = c_1 \frac{A}{\rho A_1 A_2} \quad \text{and} \quad \beta_n \to 0. \tag{13a,b}$$

In view of Eqs. (13a) and (13b), Eq. (11b) reduces to

$$(\omega_{n2})^2 \to \alpha_n = c_1 \frac{A}{\rho A_1 A_2} \quad \text{or} \quad \Omega_{n2} \to \sqrt[4]{c_1 \frac{A^2 L^4}{A_1 A_2 EI}}. \tag{14}$$

It can be seen that ω_{n2} is constant for given values of c_1, ρ, A_1 and A_2. Under the aforementioned conditions, this second set of frequencies is independent of the large magnitudes of length L, mode number n and the end conditions. The frequency value is only dependent on the van der Waals force coefficients c_1 and the diameters of the tubes. To verify the above observation, the results based on Eq. (14) are compared to those based on

Eq. (11b) for large L/d and small n values. It is found that they are in excellent agreement. However, the allowance for shear deformation and rotary inertia lowers the second set of frequency values when the mode number is large.

If L/d increases to 50 (i.e. the beam becomes longer and more slender), the influence of the shear deformation and rotary inertia on the higher n-order resonant frequencies Ω_{n2} can be neglected (Fig. 4c). It is also observed from Fig. 4c that Ω_{n2} is insensitive to the mode number. As for the lower frequency set Ω_{n1}, the results obtained by the Timoshenko beam model agree well with those obtained by the Euler beam model for the first few modes, say $n \leqslant 10$. However, as n becomes larger, the frequencies separate with the Timoshenko beam model furnishing lower results than those of the Euler beam due to shear deformation and rotary inertia.

To obtain a better insight into the effects, the relative percentage difference $\Psi = |\Omega^{\mathrm{T}} - \Omega^{\mathrm{E}}/\Omega^{\mathrm{E}}| \times 100\%$ of the two resonant frequencies are plotted in Fig. 6, where Ω^{T} and Ω^{E} represent the frequencies of DTB and DEB models, respectively. The percentage difference of Ω_{n2}, denoted by solid line is very small with only a maximum value of 1.35% at $n = 15$. In contrast, the percentage difference is very large for Ω_{n1} since Ω_{n1} is sensitive to mode number, length-to-diameter ratio and end conditions. The percentage difference is proportional to the mode number. This implies that the shear deformation and rotary inertia have greater influence on the lower set of frequencies Ω_{n1} than the higher set of Ω_{n2}.

When $L/d > 100$, the results shown in Fig. 4d reveal that DTB and DEB results are almost equivalent. So for long and slender CNTs, shear deformation and rotary inertia have negligible effect on the vibration frequencies.

As can be seen in Table 3, the first several frequencies Ω_{n1} ($n \leqslant 7$) of DTB and DEB model for double-walled CNT with CC end conditions are close to those given by SEB model, especially when L/d is 50 and beyond. The first several Ω_{n1} for CNT with large L/d can therefore be estimated by the SEB model instead of DTB or DEB with good accuracy.

Similar observations are made for double-walled CNTs with other boundary conditions, such as simply supported (SS) and clamped-simply supported (CS) ends. Sample vibration results are presented in Tables 4 and 5 for these boundary conditions. It can be observed from Tables 4 and 5 as well as from Figs. 4 and 5 that the higher set of frequencies Ω_{n2} for the above four different end conditions are close to each other, i.e. approximately 63.5 for $L/d = 50$. In conclusion, the higher set of frequencies Ω_{n2} is insensitive to end conditions, mode number and length. On the other hand, the lower set of frequencies Ω_{n1} is sensitive to the aforementioned factors. It is also shown that the transverse shear deformation and rotary inertia have greater influence on Ω_{n1} than Ω_{n2}. Furthermore, these effects are proportional to the mode number.

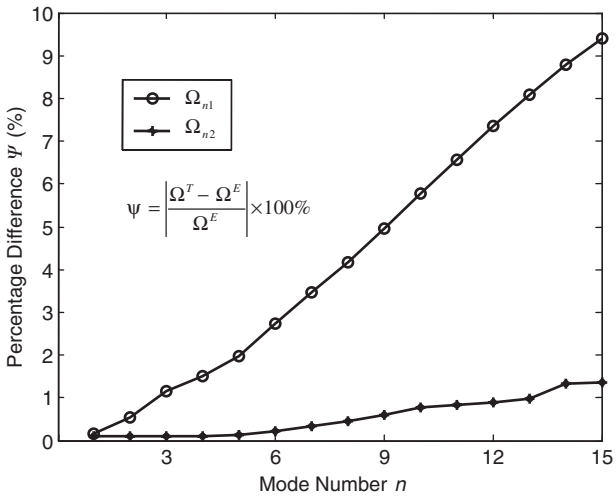

Fig. 6. Percentage difference between frequencies of DEB and DTB models ($L/d = 50$).

Table 3
Comparison of lower frequency parameters between DTB, DEB and SEB models with CC end conditions

n	$L/d = 30$ Ω_{n1}		$L/d = 50$ Ω_{n1}		$L/d = 100$ Ω_{n1}		SEB
	DTB	DEB	DTB	DEB	DTB	DEB	
1	4.7112	4.7123	4.7224	4.7300	4.7328	4.7300	4.7300
2	7.7189	7.8533	7.8119	7.8539	7.8208	7.8539	7.8540
3	10.663	10.992	10.868	10.995	11.020	10.995	10.995
4	13.597	14.124	13.922	14.135	14.137	14.137	14.137
5	16.369	17.244	16.932	17.274	17.125	17.278	17.279
6	18.988	20.338	19.850	20.410	20.292	20.420	20.420
7	21.519	23.391	22.727	23.541	23.430	23.561	23.562
8	23.968	26.373	25.552	26.664	26.423	26.701	26.703
9	26.258	29.247	28.298	29.775	29.467	29.841	29.845
10	28.444	31.962	30.976	32.870	32.496	32.980	32.987

Table 4
Frequency parameters of double-walled CNT modeled by DTB and DEB models with SS end condition

n	$L/d = 10$				$L/d = 50$			
	Ω_{n1}		Ω_{n2}		Ω_{n1}		Ω_{n2}	
	DTB	DEB	DTB	DEB	DTB	DEB	DTB	DEB
1	3.0662	3.1410	12.700	12.720	3.1438	3.1416	63.485	63.560
2	6.0378	6.2650	12.714	12.843	5.8453	6.2832	63.490	63.561
3	8.5758	9.2756	12.805	13.381	9.3509	9.4245	63.502	63.565
4	10.850	11.880	13.846	14.832	12.536	12.565	63.517	63.576
5	13.115	13.946	15.016	17.383	15.726	15.705	63.522	63.601
6	14.5924	15.941	17.532	20.458	18.020	18.843	63.541	63.645
7	16.0989	18.071	18.893	23.696	21.095	21.976	63.555	63.72
8	16.470	20.319	20.195	26.993	25.101	25.103	63.578	63.829
9	18.039	22.645	21.192	30.316	28.055	28.221	63.687	63.991
10	19.512	25.020	22.064	33.653	30.913	31.325	63.855	64.217

Table 5
Frequency parameters of double-walled CNT modeled by DTB and DEB models with CS end condition

n	$L/d = 10$				$L/d = 50$			
	Ω_{n1}		Ω_{n2}		Ω_{n1}		Ω_{n2}	
	DTB	DEB	DTB	DEB	DTB	DEB	DTB	DEB
1	3.8598	3.9253	11.788	12.732	3.9156	3.9270	62.596	63.560
2	6.7185	7.0355	12.705	12.923	7.0505	7.0685	63.485	63.561
3	9.2148	9.9811	12.803	13.636	10.179	10.210	63.491	63.567
4	11.344	12.432	13.396	15.384	13.227	13.350	63.501	63.581
5	13.078	14.436	14.858	18.125	16.309	16.490	63.515	63.609
6	14.013	16.460	16.890	21.259	19.318	19.626	63.526	63.660
7	15.337	18.623	18.410	24.516	22.218	22.759	63.542	63.741
8	16.233	20.894	19.856	27.822	25.123	25.884	63.555	63.864
9	17.601	23.235	21.236	31.149	27.923	28.999	63.578	64.041
10	18.935	25.619	21.596	34.489	30.673	32.098	63.813	64.285

4. Conclusions

Single and multi-walled Timoshenko beam models are developed for the free vibration of CNTs with various end conditions. The models allow for the effects of transverse shear deformation and rotary inertia. For a STB model, it is found that the aforementioned effects lead to a decrease in frequencies when compared to those obtained by the Euler beam model. This phenomenon is amplified at higher mode numbers and for small length-to-diameter ratios. With increasing length-to-diameter ratios, the effects of shear deformation and rotary inertia on the frequencies diminish and the results given by the Timoshenko beam model are equivalent to those of the Euler beam model. The STB model, similar to its Euler counterpart, treats the MWNTs as a single beam. The frequencies for CNTs with large L/d can be estimated by the single beam model with reasonably good accuracy. However, it fails to capture the intertube relative vibration of MWNTs and hence the model is not good for predicting frequencies of CNTs with small L/d and higher order frequencies. Furthermore, it only provides one set of frequencies when there should be N sets of frequencies equal to the N walls in a MWNT.

For a double-walled CNT modeled by a DTB model, there are two sets of n-order resonant frequencies due to non-coaxial vibration. The allowance for shear deformation and rotary inertia in the Timoshenko beam has a greater effect on the lower set of n-order resonant frequency than the higher set. The phenomenon is clearly seen when the mode numbers are large.

This study focuses on the free vibration of CNTs. Research is underway to extend the present multi-Timoshenko beam model for the buckling and post-buckling problems of CNTs.

Appendix A. DQ weighting coefficients

Given the coordinates of M grid points as calculated from Eq. (2), the weighting coefficients a_{ij} and b_{ij} of the first- and second-order derivatives with respect to x, respectively, are given by Timoshenko [30]

$$a_{ij} = \frac{1}{(x_j - x_i)} \prod_{\substack{k=1 \\ k \neq i,j}}^{M} \frac{x_j - x_k}{x_j - x_i}, \quad i,j = 1,2,\ldots,M, \quad i \neq j, \tag{A.1}$$

$$a_{ii} = -\sum_{\substack{j=1 \\ j \neq i}}^{M} a_{ij}, \quad i = 1,2,\ldots,M, \tag{A.2}$$

$$b_{ij} = 2\left[a_{ij}a_{ii} - \frac{a_{ij}}{x_j - x_i}\right], \quad i,j = 1,2,\ldots,M, \quad i \neq j, \tag{A.3}$$

$$b_{ii} = -\sum_{\substack{j=1 \\ j \neq i}}^{M} b_{ij}, \quad i = 1,2,\ldots,M. \tag{A.4}$$

References

[1] S. Iijima, Helical microtubules of graphitic carbon, *Nature* 354 (1991) 56–58.
[2] M.M.J. Treacy, T.W. Ebbesen, J.M. Gibson, Exceptionally high Young's modulus observed for individual carbon nanotubes, *Nature* 381 (1996) 678–680.
[3] J. Bernholc, C. Brabec, M.B. Nardelli, A. Maiti, C. Roland, B.I. Yakobson, Theory of growth and mechanical properties of nanotubes, *Applied Physics A—Materials Science and Processing* 67 (1998) 39–46.
[4] R.H. Baughman, et al., Carbon nanotubes actuators, *Science* 284 (1999) 1340–1344.
[5] M.F. Yu, O. Lourie, M.J. Dyer, K. Moloni, T.F. Kelly, R.S. Ruoff, Strength and breaking mechanism of multiwalled carbon nanotubes under tensile load, *Science* 287 (2000) 637–640.
[6] C.Q. Ru, Elastic models for carbon nanotubes, *Encyclopedia of Nanoscience and Nanotechnology* X (2003) 1–14.

[7] B.I. Yakobson, C.J. Brabec, J. Bernholc, Nanomechanics of carbon tubes: instabilities beyond linear response, *Physical Review Letters* 76 (1996) 2511–2514.
[8] B.I. Yakobson, R.E. Smalley, Fullerene nanotubes: C-100000 and beyond, *American Scientist* 85 (1997) 324–337.
[9] S. Govindjee, J.L. Sackman, On the use of continuum mechanics to estimate the properties of nanotubes, *Solid State Communications* 110 (1999) 227–230.
[10] J. Yoon, C.Q. Ru, A. Mioduchowski, Vibration of an embedded multiwall carbon nanotube, *Composites Science and Technology* 63 (2003) 1533–1542.
[11] C.Q. Ru, Effect of van der Waals forces on axial buckling of a double-walled carbon nanotube, *Journal of Applied Physics* 87 (2000) 1712–1715.
[12] C.Q. Ru, Effective bending stiffness of carbon nanotubes, *Physical Review B* 62 (2000) 9973–9976.
[13] C.Q. Ru, Elastic buckling of single-walled carbon nanotubes ropes under high pressure, *Physical Review B* 62 (2000) 10405–10408.
[14] C.Q. Ru, Axially compressed buckling of a double-walled carbon nanotubes embedded in an elastic medium, *Journal of Mechanics and Physics of Solids* 49 (2001) 1265–1279.
[15] C.Q. Ru, Degraded axial buckling strain of multiwalled carbon nanotubes due to interlayer slips, *Journal of Applied Physics* 89 (2001) 3426–3433.
[16] C.Y. Li, T.W. Chou, A structural mechanics approach for the analysis of carbon nanotubes, *International Journal of Solids and Structures* 40 (2003) 2487–2499.
[17] C.Y. Li, T.W. Chou, Vibrational behaviors of multiwalled-carbon-nanotube-based nanomechanical resonators, *Applied Physics Letters* 84 (2004) 121–123.
[18] P. Poncharal, Z.L. Wang, D. Ugarte, W.A. De Heer, Electrostatic deflections and electromechanical resonances of carbon nanotubes, *Science* 283 (1999) 1513–1516.
[19] J. Yoon, C.Q. Ru, A. Mioduchowski, Non-coaxial resonance of an isolated multiwall carbon nanotube, *Physical Review B* 66 (2002) 233402–233414.
[20] V.N. Popov, V.E.N. Doren, Elastic properties of single-walled carbon nanotubes, *Physics Review B* 61 (2000) 3078–3084.
[21] J. Yoon, C.Q. Ru, A. Mioduchowski, Sound wave propagation in multiwall carbon nanotubes, *Journal of Applied Physics* 93 (2003) 4801–4806.
[22] J. Yoon, C.Q. Ru, A. Mioduchowski, Timoshenko-beam effects on transverse wave propagation in carbon nanotubes, *Composites: Part B* 35 (2004) 87–93.
[23] E.W. Wong, P.E. Sheehan, C.M. Lieber, Nanobeam mechanics: elasticity, strength, and toughness of nanorods and nanotubes, *Science* 277 (1997) 1971–1975.
[24] M.R. Falvo, G.J. Clary, R.M. Taylor, V. Chi, F.P. Brooks, S. Washburn, et al., Bending and buckling of carbon nanotubes under large strain, *Nature* 389 (1997) 582–584.
[25] N.G. Chopra, A. Zettl, Measurement of the elastic modulus of multiwall boron nitride nanotubes, *Solid State Communications* 105 (1998) 297–300.
[26] P. Kim, C.M. Lieber, Nanotube nanotweezers, *Science* 286 (1999) 2148–2150.
[27] H.J. Dai, J.H. Hafner, A.G. Rinzler, D.T. Colbert, R.E. Smalley, Nanotubes as nanoprobes in scanning probe microscopy, *Nature* 384 (1996) 147–150.
[28] E.S. Snow, P.M. Campbell, J.P. Novak, Single-wall carbon nanotubes atomic force microscope probes, *Applied Physics Letters* 80 (2002) 2002–2004.
[29] E.S. Snow, P.M. Campbell, J.P. Novak, Atomic force microscopy using single-wall C nanotubes probes, *Journal of Vacuum Science & Technol.ogy B* 20 (2002) 822–827.
[30] S.P. Timoshenko, *Vibration Problems in Engineering*, Wiley, New York, 1974.
[31] T.M. Wang, J.E. Stephens, Natural frequencies of Timoshenko beams on Pasternak foundations, *Journal of Sound and Vibration* 51 (1977) 149–155.
[32] C. Shu, *Differential Quadrature and Its Application in Engineering*, Springer, Berlin, 2000.
[33] H.P. William, A.T. Saul, T.V. William, P.F. Brian, *Numerical Recipes in FORTRAN*, Cambridge, UK, 1992.
[34] I.H. Shames, C.L. Dym, *Energy and Finite Element Methods in Structural Mechanics*, Hemisphere, Washington, DC, 1985.
[35] C.Q. Ru, Column buckling of multiwalled carbon nanotubes with interlayer radial displacements, *Physics Review B* 62 (2000) 16962–16967.